J Mol Model (2009) 15:623–631
DOI 10.1007/s00894-008-0383-z

ORIGINAL PAPER

Design of laser pulses for selective vibrational excitation of the N6-H bond of adenine and adenine-thymine base pair using optimal control theory

Sitansh Sharma · Purshotam Sharma · Harjinder Singh · Gabriel G. Balint-Kurti

Received: 1 September 2008 / Accepted: 29 October 2008 / Published online: 5 December 2008

Abstract Time dependent quantum dynamics and optimal control theory are used for selective vibrational excitation of the N6-H (amino N-H) bond in free adenine and in the adenine-thymine (A-T) base pair. For the N6-H bond in free adenine we have used a one dimensional model while for the hydrogen bond, N6-H(A)...O4(T), present in the A-T base pair, a two mathematical dimensional model is employed. The conjugate gradient method is used for the optimization of the field dependent cost functional. Optimal laser fields are obtained for selective population transfer in both the model systems, which give virtually 100% excitation probability to preselected vibrational levels. The effect of the optimized laser field on the other hydrogen bond, N1(A)...H-N3(T), present in A-T base pair is also investigated.

Keywords Conjugate gradient method · Cost functional · Free adenine · Hydrogen bonded A-T · Optimal control · Vibrational control

PACS 31.50.Bc · 33.20.Tp · 82.39.Pj · 82.37.Rs · 82.50.Bc · 82.50.Nd

S. Sharma · P. Sharma · H. Singh (✉)
Center for Computational Natural Sciences and Bioinformatics,
International Institute of Information Technology,
Hyderabad 500032, India
e-mail: laltu@mail.iiit.ac.in

G. G. Balint-Kurti
Centre for Computational Chemistry and School of Chemistry,
University of Bristol,
Bristol BS8 1TS, UK
e-mail: Gabriel.Balint-Kurti@bristol.ac.uk

Introduction

Controlling dynamics at the atomic level is a primary goal of chemists. Optimal control theory (OCT) [1–17] has emerged as a comprehensive tool for designing laser pulses to achieve prescribed dynamical goals. The objective of the theory is to find laser fields which will transform the nuclear wavefunction (or density matrix) of a system from an initial state to a desired final state by using time-dependent quantum mechanical propagation in combination with an optimization algorithm. Control of biological molecules using OCT is quite difficult because of their inherently complex dynamical properties. The development of laser pulse shaping techniques has opened the way to achieving this goal [18–21].

The role of hydrogen bonds in determining the three-dimensional structures of biomolecules like proteins and nucleic acids is well established. Vibrational analysis of hydrogen bonded systems provides information about the nature of the local interactions as well as the dynamics and coupling of nuclear motion [22]. Studies on the control of vibrational quantum dynamics of hydrogen bonded sites in these biomolecules using optimally designed laser pulses will provide greater insights into their dynamical behavior. Ohmura et al. [23] demonstrated the use of lasers to control photodissociation of ternary aniline cluster cations consisting of aniline, water and an aromatic molecule (benzene or pyrrole). They utilized the strong interaction between N-H stretching vibration and adjacent hydrogen bond for control of photodissociation. Villani et al. [24–26] considered the time-dependent interaction among the DNA base pairs and performed laser control studies on hydrogen transfer in adenine-thymine and guanine-cytosine base pairs.

We have used OCT to design infrared laser pulses for selective vibrational excitation of the N6-H bond present in

two different molecular environments. One in the free adenine molecule and the second in the hydrogen bonded state N6-H(A)...O4(T) present in A-T base pair. We are interested in finding the difference in the nature of the laser fields needed to excite N-H stretching when the molecule is in its free state and when it is involved in hydrogen bonding. For the free N6-H(A) system present in adenine, we have used a one dimensional model while for N-H in its hydrogen bonded state, i.e., N6-H(A)...O4(T), a two mathematical dimensional model is employed. Density functional theory is used to obtain the potential energy and dipole moment plots for both the systems. Optimized laser fields are realized which give virtually 100% excitation probability to preselected vibrational levels. In this work we are presenting our results for the following vibrational excitations:

1) N6-H in adenine molecule (Free state):
a) v=0 to v=1
b) v=1 to v=2
c) v=0 to v=2
2) N6-H in hydrogen bonded state (N6-H(A)...O4(T)) in A-T base pair:
a) v=0 to v=12 (corresponds to one node in N6-H(A) mode)
b) v=12 to v=33 (corresponds to two nodes in N6-H(A) mode)
c) v=12 to v=37 (corresponds to one node in H(A)...O4 (T) and two nodes in N6-H(A) mode).

In the transition v=12 to v=37 we are looking for a laser field which will displace the inter-base hydrogen so that it moves closer to the oxygen of thymine. The paper is organized as follows: In Electronic structure calculations and models, we present the details of electronic structure calculations and the description of the simple control models. In Optimal control theory, the optimal control formulation is described in detail. Optimization method describes the conjugate gradient method, used for optimization of the cost functional constructed in Optimal control theory. In Results and discussion, the numerical results obtained by OCT are presented and discussed, while concluding remarks are given in Conclusions.

Theory and method

Electronic structure calculations and models

For our studies we have considered the hydrogen bond between amino N6-H of adenine and oxygen (O4) of thymine in A-T base pair. We have modeled the hydrogen bonded system using two dimensional Jacobi coordinate representation as shown in Fig. 1(b).

In order to construct the potential energy and dipole moment surfaces for this model we have used the structures optimized at RI-MP2 (resolution of identity) method with aug-cc-pVTZ basis set of atomic orbitals from an earlier study by Šponer et al. [27]. Density functional theory with the popular B3LYP hybrid exchange-correlation functional is used to obtain the potential energy and dipole moment surfaces shown in Fig. 2. For oxygen, nitrogen and carbon we have used the 6-31G** basis set while the aug-cc-pvdz basis was used for the hydrogen atom.

Similarly for the amino N6-H bond present in free adenine we have used a one dimensional model shown in Fig. 1(c). The potential energy and dipole moment curves for amino N6-H bond of adenine are calculated by varying the N6-H bond distance keeping the rest of the molecule fixed at the same level of theory and using the same basis sets. All the ab initio electronic structure calculations are performed using the Gaussian03 suite [28] of quantum chemical programs.

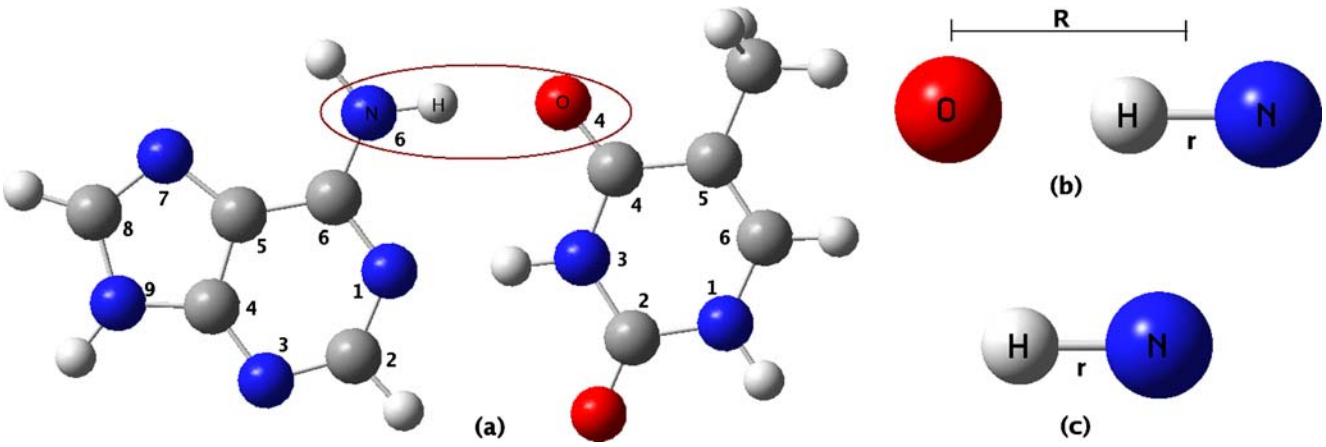

Fig. 1 (a) Optimized geometry of A-T base pair at RIMP2/aug-cc-pVTZ level (numbers shown are the same as standard numbering used for nucleobases.); (b) Two dimensional representation of triatomic N6-H(A)...O4(T) (circled in (a)), where R = distance of O4 from center of mass of N6-H(A) and r = bond length of N6-H bond; (c) One dimensional representation of diatomic amino N6-H in free adenine, where r = bond length of N6-H bond

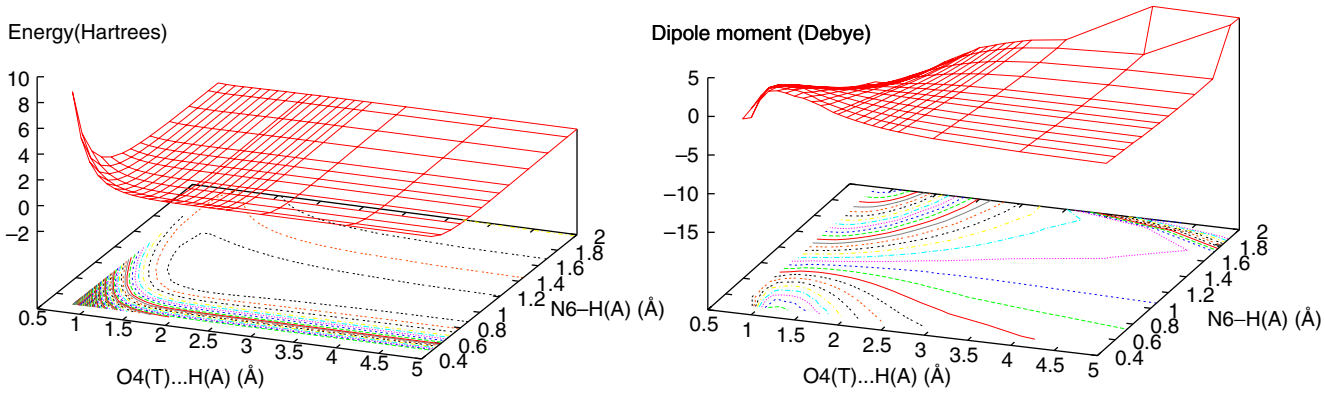

Fig. 2 Variation in potential energy and x-component (μ_x) of dipole moment with change in the bond lengths of O4(T)...H(A) and N6-H(A) bonds, obtained using DFT

Optimal control theory

The time evolution of the molecular wavefunction $|\psi(t)\rangle$ is governed by the time-dependent Schrödinger equation (atomic units used throughout the paper, $\hbar=1$)

$$i\frac{\partial}{\partial t}|\psi(t)\rangle = \widehat{H}|\psi(t)\rangle = \left[\widehat{H}_0 + \widehat{H}_1(t)\right]|\psi(t)\rangle, \tag{1}$$

where $\widehat{H}_0$ is the system Hamiltonian and $\widehat{H}_1(t)$ is the interaction Hamiltonian, respectively. The interaction Hamiltonian $\widehat{H}_1(t)$ for the system under the influence of an external field, $\epsilon(t)$, within dipole approximation, can be defined as

$$\widehat{H}_1(t) = -\widehat{\mu}\varepsilon(t) \tag{2}$$

where $\widehat{\mu}$ is the dipole moment operator.

In the OCT formalism, we construct a field dependent functional. This functional contains our objective term which is the overlap of the field propagated initial wavefunction with target wavefunction, a penalty term for the fluence which restricts the undesirable physical processes during the controlled evolution of the molecule and the dynamical constraint that the time-dependent Schrödinger equation be obeyed at all time. The overall grand cost functional to be optimized takes the following shape:

$$J[\epsilon(t)] = \left|\langle\psi_i(T)|\phi_f\rangle\right|^2 - \alpha_0\int_0^T[\epsilon(t)]^2dt - 2\quad Re \tag{3}$$
$$\left[\int_0^T\left\langle\chi_f(t)\right|\frac{\partial}{\partial t} + i\widehat{H}(\epsilon(t))|\psi_i(t)\right\rangle dt\Bigg],$$

here, ϵ(t) is the electric-field strength as a function of time; ψ_i(t) is the initial wavefunction propagated to time T under the action of the optimal laser field ϵ(t); ϕ_f is the target state to be reached at the final time T; α_0 is a constant positive weighting parameter that specifies the weight of the fluence term in the functional; and $\chi_f(t)$ is a Lagrange multiplier introduced to assure satisfaction of the time-dependent Schrödinger equation.

Varying the grand functional (Eq. (3)) with respect to the wavefunction, $\psi_i(t)$, the Lagrange multiplier, $\chi_f(t)$, and the electric field, $\epsilon(t)$, leads to the following set of nonlinear pulse design equations for selective vibrational excitation :

$$i\frac{\partial\psi_i(t)}{\partial t} = \widehat{H}\psi_i(t), \quad \psi_i(0) = \phi_i, \tag{4}$$

$$i\frac{\partial\chi_f(t)}{\partial t} = \widehat{H}\chi_f(t), \quad \chi_f(T) = \langle\phi_f|\psi_i(T)\rangle\phi_f, \tag{5}$$

$$\alpha_0\epsilon(t) = \mathrm{Im}\left(\left\langle\chi_f(t)\right|\frac{\partial}{\partial\epsilon(t)}\widehat{H}\left|\psi_i(t)\right\rangle\right). \tag{6}$$

The nature of these coupled differential equations demands that they be solved iteratively. In order to maximize the cost functional we calculate the derivative of the functional with respect to a variation of the electric field at time t and use the conjugate-gradient method. The method is explained in more detail in the next section.

Optimization method

In order to find the optimal laser field for a specific vibrational excitation by maximizing the cost functional subjected to Eqs. 4 and 5, we employed the conjugate gradient method [8–10]. We define the laser field $\epsilon(t)$ as having two parts: a Gaussian envelope function $s(t)$, which is practically zero at t=0 and at t = T and a part $\epsilon_0(t)$ which will be optimized to achieve the desired objective, i.e.,

$$\epsilon(t) = s(t)\epsilon_0(t) \tag{7}$$

here, $s(t) = e^{\frac{-(t-T/2)^2}{(T/4)^2}}$, which is preserved throughout the optimization to ensure smooth switch on and off of the electric field.

The gradient of J with respect to small variation in ϵ_0 at time t after k number of iterations in the optimization cycle is written as

$$g^k(t) = \frac{\partial J^k}{\partial \epsilon_0^k(t)} = -2s(t)\left[\alpha_0 \epsilon^k(t) - \mathrm{Im}\left\langle \chi_f(t)\left|\frac{\partial \widehat{H}}{\partial \epsilon^k(t)}\right|\psi_i(t)\right\rangle\right]. \tag{8}$$

The molecular wave function, $\psi_i(t)$, and the Lagrange multiplier, $\chi_f(t)$, are propagated in time using the second order split-operator method [29, 30]. A line search along the Polak-Ribiere-Polyak search direction is now performed. The search direction is defined using the gradients given in Eq. 8:

$$d^k(t_i) = g^k(t_i) + \frac{\sum_i g^k(t_i)^T\left(g^k(t_i) - g^{k-1}(t_i)\right)}{\sum_i g^{k-1}(t_i)^T g^{k-1}(t_i)} d^{k-1}(t_i) \tag{9}$$

where k=2, 3, ..., and $d^1(t_i) = g^1(t_i)$. To prevent the algorithm from sampling $\epsilon(t)$ values outside of the predefined electric-field amplitude range during the line search, the direction $d^k(t)$ is projected. The projected search direction is Fourier transformed to obtain a function of frequency, and this function is filtered using a 20th-order Butterworth bandpass filter in order to restrict the frequency components of the electric field within a specified range. The updated electric-field is expressed as

$$\epsilon^{k+1}(t) = \epsilon^k(t) + \lambda s(t) d_p^k(t), \tag{10}$$

where λ is determined by the line search.

Results and discussion

We discuss the results obtained using optimal control formalism described above for the model systems constructed for free adenine and A-T base pair. For all the transitions we have propagated the system using laser pulse of length 40,000 $\hbar/E_h$, which was discretized into 16384 points. The weight for the penalty term (α_0) is fixed as 0.1 in all the calculations.

Vibrational control of N6-H in free adenine (one dimensional model)

For the one dimensional model we have designed the laser pulses for three vibrational excitations. The first transition is the fundamental transition from the ground vibrational state to the first excited vibrational state (v=0 to v=1). The second transition is an excitation from the first excited vibrational state to the second excited vibrational state (v=1 to v=2) and third transition is an excitation from the ground vibrational state to the second excited vibrational state (v=0 to v=2). The Fourier grid Hamiltonian method (FGHM) [31] is employed to calculate the vibrational spectrum for the one dimensional N6-H system.

a) Transition v=0 to v=1: For this fundamental transition the initial guess field is chosen as: $\epsilon(t)$=0.0012 sin $(\omega_{0,1}t)s(t)$ where $\omega_{0,1}$ is transition frequency from v=0 to v=1 and $s(t) = e^{\frac{-(t-T/2)^2}{(T/4)^2}}$. The optimized electric field is shown in plot a1 and its corresponding frequency components are shown in plot a2 of Fig 3. Plot a2 shows a major peak around 3547 cm^{-1}. Plot a3 shows the population variation with time of the various states involved during the transition. It shows that the population in initial state v=0 decreases with time while that of target state v=1 increases. There is some population transfer to higher vibrational state v=2 also, but in the end of pulse whole of the population is transferred to v=1. The convergence behavior of the cost functional, J, and the transition probability, $\left|\langle\psi_i(T)|\phi_f\rangle\right|^2$, versus the number of iteration steps is shown in plot a4. The convergence of the algorithm is found to be very fast. After only a few iteration steps, the final cost functional is more than 97% of its maximum value. It is seen that the transition probability reaches nearly 100%.

b) Transition v=1 to v=2: Initial guess field chosen for the optimization is $\epsilon(t)$=0.001 sin$(\omega_{1,2}t)s(t)$ where $\omega_{1,2}$ is the transition frequency from v=1 to v=2 and s(t) is the same as for the above transition. The plot b1 shows the optimized field and its amplitude, which is less than the amplitude of the optimized field for transition v=0 to v=1. The power spectra of optimized field (plot b2 of Fig. 3) shows that the major frequency peak is around 3386 cm^{-1}. The populations of the field propagated initial state, target state and other vibrational states with time are shown in plot b3 of Fig. 3. The plot b4 of the cost functional and transition probability against number of iterations shows that, after only a few iterations, both have reached values of more than 98% of their maximum values.

c) Transition v=0 to v=2: For this transition the initial guess field is chosen as: $\epsilon(t) = 0.005\sin\left(\frac{\omega_{0,2}}{2}t\right)s(t)$ where $\frac{\omega_{0,2}}{2}$ is half of the transition frequency from v=0 to v=2 and s(t) is the same as for the above transition. The optimized field and its corresponding frequency spectra are shown in plots c1 and c2 of Fig. 3. The shape of the field shows that there are a number of subpulses, which is confirmed by its frequency plot c2. It shows two major frequency components in the field, one corresponds to the transition frequency from v=0 to v=1 while other corresponds to transition frequency from v=1 to v=2. The mechanism of population transfer

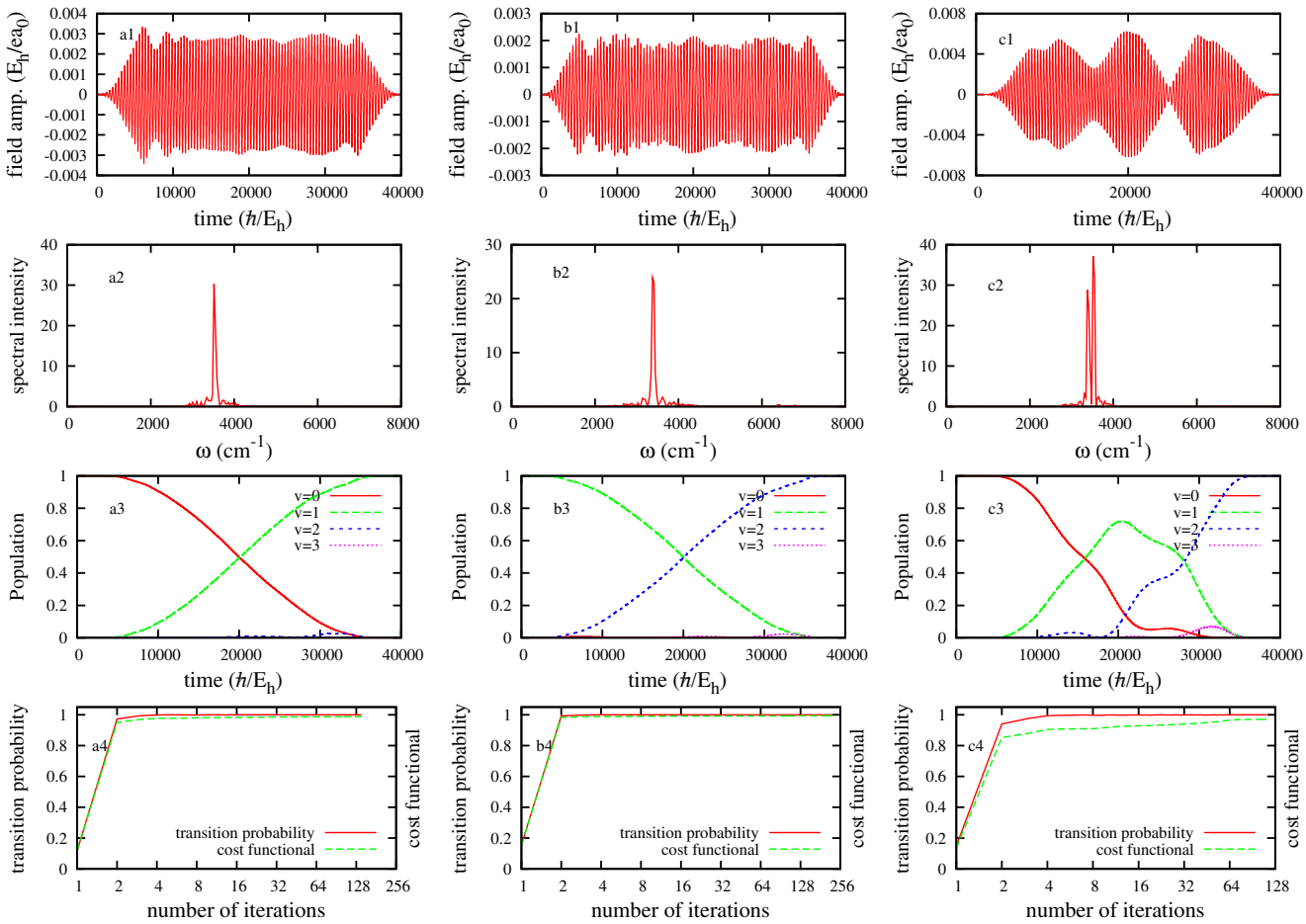

Fig. 3 Results for transitions v=0 to v=1, v=1 to v=2 and v=0 to v=2 for free adenine: (a1, b1, c1) optimized laser field, (a2, b2, c2) its frequency distribution, (a3, b3, c3) populations of different states as a function of time and (a4, b4, c4) convergence behavior of the transition probability and the cost functional, J, with number of iterative steps involved in the optimization

can be described from plot c3 which shows the population variation in various vibrational states with time involved during the transition. This plot shows that first the population is transferred from v=0 to v=1 and then in the middle of the pulse population starts transferring from v=1 to higher vibrational states. At the end of the pulse whole of the population is in target state v=2. The involvement of intermediate states in population transfer indicates complex dynamical behavior of the system. Variation of cost functional and transition probability with number of iterations is plotted in plot c4.

Vibrational control of amino N6-H(A)...O4(T) in A-T (two dimensional model)

As discussed in Theory and method, for these studies we are considering N6-H(A)...O4(T) hydrogen bond present in the adenine-thymine base pair. The Fourier Grid Hamiltonian method (FGHM) is employed to create a direct product basis for the variational calculation of the triatomic wave functions of the N6-H(A)...O4(T) system. Some of the wavefunctions obtained after bound state analysis are plotted in Fig. 4. For the time propagation, we used 64 grid points for both R and r coordinates. In order to investigate the difference in the nature of fields for amino N6-H in free adenine and in hydrogen bonded state we considered three transitions. The first transition is from the ground vibrational state to the vibrational state corresponding to N6-H stretching (v=0 to v=12). The second transition is between the first excited N6-H stretching vibrational mode and the second excited mode (v=12 to v=33). In the last transition we considered v=12 to be our initial state and v=37 to be the target state.

a) Transition v=0 to v=12: The initial guess field employed is $\epsilon(t)=0.00043\ \sin(\omega_{0,12}t)s(t)$ where $\omega_{0,12}$ is the transition frequency from v=0 to v=12 and s(t) is the same as for the earlier case. The plot a1 in Fig. 5

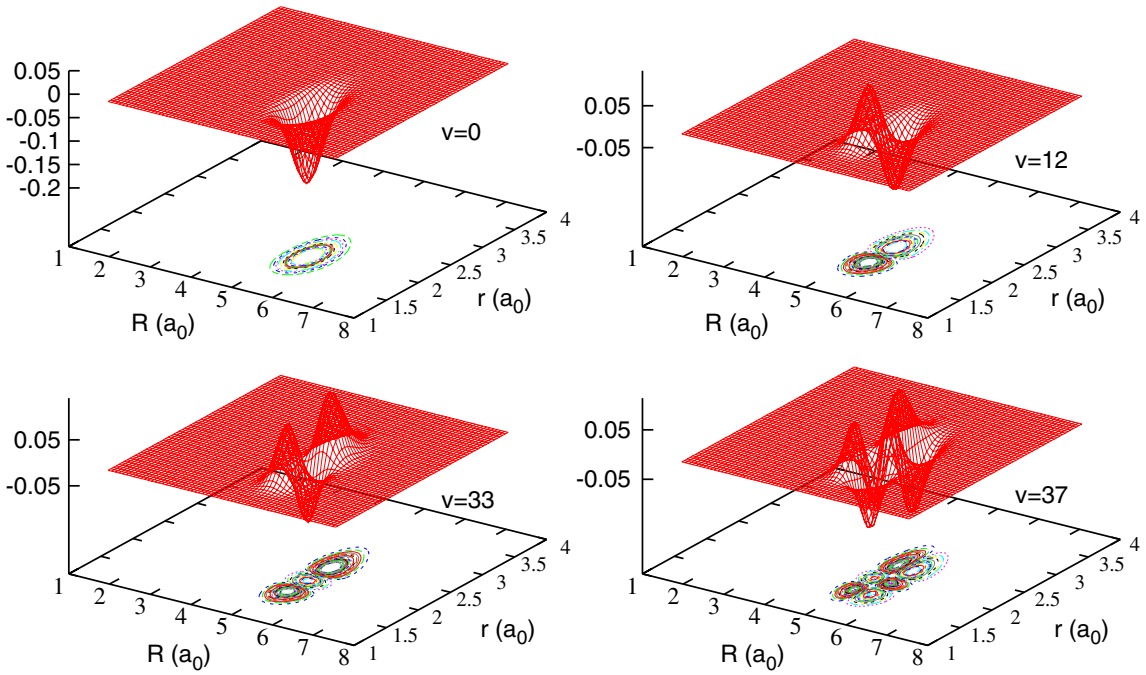

Fig. 4 Wavefunctions for the control system N6-H(A)...O4(T) of the A-T base pair obtained after bound state calculations using FGHM

shows the optimized field for the transition. The maximum amplitude of the field is 0.000423 $\frac{E_h}{ea_0}$. The corresponding frequency analysis in plot a2 of Fig. 5 shows a major peak around 3162 cm^{-1}. This frequency is less than the frequency of corresponding mode in free adenine amino bond. Because of elongation of N6-H bond in the hydrogen bonded system (N6-H(A)...O4(T)), the force constant of this bond has decreased as compared to free adenine amino bond. Moreover, the maximum amplitude of the field in the hydrogen bonded system N6-H(A)...O4(T) is less as compared to free amino bond because of larger transition dipole moment value. The smooth population transfer from v=0 to v=12 is shown in plot a3. As the time increases the population in v=0 state decreases while that in v=12 state increases. The convergence behavior of the cost functional, J, and the transition probability, $\left|\langle\psi_i(T)|\phi_f\rangle\right|^2$ versus the number of iteration steps is shown in plot a4. After only a few iteration steps, the cost functional and the transition probability has attained a value of more than 99% of its maximum.

b) Transition v=12 to v=33: From the plots of the wavefunctions we found that v=33 state corresponds to no nodes in the coordinate R and two nodes in the r coordinate (higher state in N6-H vibrational mode). So, we selected this to be our target state. In this transition our aim is to design laser pulse which will excite the system from v=12 state to v=33 state. The initial trial field is set as: $\epsilon(t)$=0.0004 $\sin(\omega_{12,33}t)s(t)$ where $\omega_{12,33}$ is transition frequency from v=12 to v=33 and s(t) is the envelope factor same as before. The optimized field having maximum amplitude 0.000255 $\frac{E_h}{ea_0}$ for the transition is shown in plot b1 of Fig. 5. The frequency analysis of the field shows that the major peak is around 2936 cm^{-1}. The populations of the field propagated initial state (v=12) and of the target state (v=33) are shown in plot b3 of Fig. 5. Plot b4 shows that the cost functional and the transition probability reach more than 99% of their maximum values after only a few iterations.

c) Transition v=12 to v=37: We examine this transition because we are interested in transferring the population into a vibrational state in which the inter-base hydrogen of N6-H group present in adenine is closer to the oxygen of thymine. Plots of wavefuntions in Fig. 4 show that v=37 state corresponds to one node in the space of coordinate R and two nodes in r space. The initial guess field is set as: $\epsilon(t)$=0.0015 $\sin(\omega_{12,37}t)s(t)$ where $\omega_{12,37}$ is the transition frequency from v=12 to v=37 and s(t) is the same as before. The shape of the optimized field shown in plot c1 is quite complex, as can also be seen from its corresponding frequency plot c2. Along with a major peak at 3270 cm^{-1} some low frequency peaks also appear in the frequency spectrum. The time variation (plot c3) of population shows that with time, population in the v=12 state decreases while that in the v=37 state increases. Moreover, some low vibrational states also get populated during the excita-

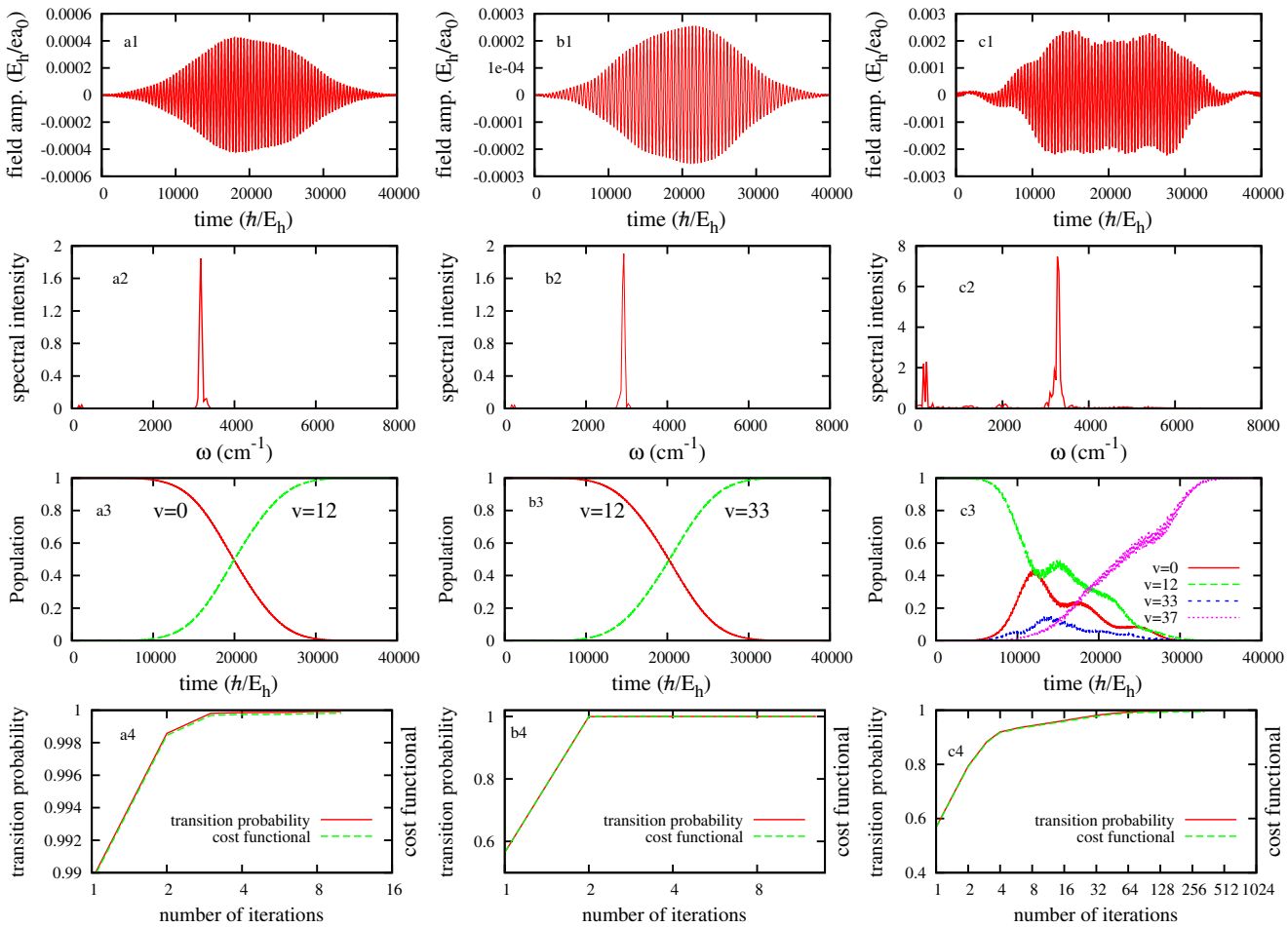

Fig. 5 Results for transitions v=0 to v=12, v=12 to v=33, v=12 to v=37 for the control system N6-H(A)...O4(T) of A-T base pair: (a1, b1, c1) optimized laser field, (a2, b2, c2) its frequency distribution, (a3, b3, c3) populations of different states as a function of time and (a4, b4, c4) convergence behavior of transition probability and the cost functional, J, with number of iterative steps involved in optimization

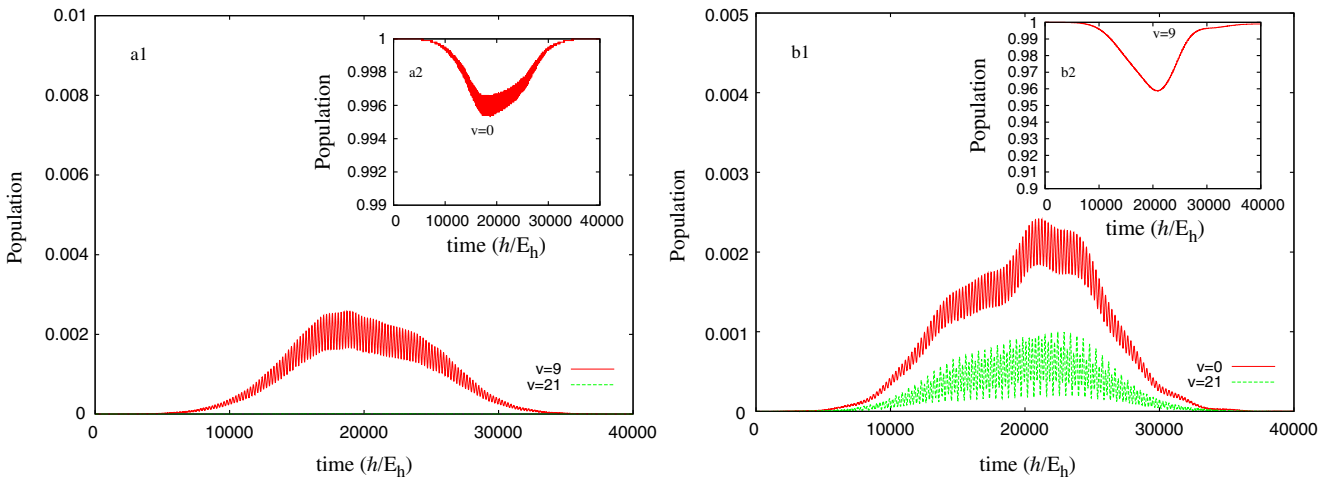

Fig. 6 Population analysis of vibrational states of N1(A)...H-N3(T) control system (another hydrogen bond) using optimized fields obtained for the control system N6-H(A)...O4(T)

tion but at the end of the pulse all of the population gets transferred to the v=37 state. The variation of the cost functional and transition probability with number of iterations is plotted in plot c4.

Effect of laser pulse on the other hydrogen bond (N1(A)...H-N3(T))

The optimized laser field designed for vibrational excitation of N6-H(A)...O4(T) may alter the population in the vibrational states of the other hydrogen bond also. In order to examine this effect, we propagated the eigenstates of N1(A)...H-N3(T) using the optimized laser pulse for excitation of the N6-H(A)...O4(T) hydrogen bond. We used a Jacobi coordinate representation for N1(A)...H-N3(T) as used for N6-H(A)...O4(T). After constructing the potential energy and dipole moment surfaces for N1(A)...H-N3(T) at the same level of theory, we employed Fourier Grid Hamiltonian method to calculate the bound states for N1(A)...H-N3(T). The wavefunction analysis for N1(A)...H-N3(T) shows that the v=9 state corresponds to one node in N3-H mode and v=21 corresponds to two nodes in N3-H mode, while having no nodes in the N1(A)...H mode. In order to examine the effect of the earlier optimized laser field (for N6-H(A)...O4(T) bond) on population of vibrational states of N1(A)...H-N3(T), we try to transfer population from v=0 to v=9 in N1(A)...H-N3(T) using the optimized field for corresponding transition v=0 to v=12 in N6-H(A)...O4(T); and from v=9 to v=21 in N1(A)...H-N3(T) using the optimized field for transition v=12 to v=33 in N6-H(A)...O4(T). The variation of population of various states with time is shown in plots a1 and a2 in Fig. 6 for v=0 to v=9. It shows that during the pulse some population is transferred from v=0 to higher states in N1(A)...H-N3(T), but the amount transferred is less then 0.004 which is almost negligible at the end of the pulse duration. Similar behavior is also observed if we used optimized field of transition v=12 to v=33 (in N6-H(A)...O4(T)) for transition v=9 to v=21 (in N1(A)...H-N3(T)) shown in plots b1 and b2 of Fig. 6. This shows that the optimized field for one of the hydrogen bond has negligible effect on the other hydrogen bond.

Conclusions

We have used optimal control theory to design laser pulses for controlling the nuclear motion in the amino bond present in free adenine and in the hydrogen bonded state in the adenine-thymine base pair. We modeled free adenine using a one dimensional N6-H model, while for the hydrogen bonded state N6-H(A)...O4(T) a two dimensional model is employed. We have discussed our results for several vibrational excitations in both the models. We also examined vibrational transitions in which the interbase hydrogen is closer to the oxygen of thymine. The peak amplitude of the fields are within reasonable and experimentally realizable bounds. Moreover, the maximum amplitudes of the optimized fields for N6-H(A)...O4(T) (hydrogen bonded state) are less than in the free adenine (N6-H) because of their large transition dipole moment value as compared to free adenine. The effect of the optimized laser fields for excitation of the N6-H(A)...O4(T) hydrogen bond on N1(A)...H-N3(T) is also investigated. The time variation of the population analysis of eigenfunctions of the N1(A)...H-N3(T) bond shows negligible population transfer into these vibrational states by the field optimized for excitation of the N6-H(A)...O4(T) hydrogen bond. Application of OCT on more refined models of this system is under investigation.

Acknowledgements We thank the Royal Society and British Council, India for supporting this work. SS and PS thank CSIR, New Delhi for research fellowships. The travel grants from DST (for SS) and DBT (for PS) for attending MDMM-2008, Piechowice, Poland are greatfully acknowledged.

References

1. Rice S, Zhao M (2000) Optical control of molecular dynamics. Wiley-Interscience, New York
2. Shapiro M, Brumer P (2003) Principles of the quantum control of molecular processes. Wiley-Interscience, New York
3. Ohtsuki Y, Nakagami K, Fujimura Y (2001) J Chem Phys 114:8867–8876
4. Tannor DJ, Rice SA (1985) J Chem Phys 83:5013–5018
5. Tannor DJ, Kosloff R, Rice SA (1986) J Chem Phys 85:5805–5820
6. Tannor DJ, Rice SA (1988) Adv Chem Phys 70:441–523
7. Nuernberger P, Vogt G, Brixner T, Gerber G (2007) Phys Chem Chem Phys 9:2470–2497
8. Balint-Kurti GG, Manby FR, Ren Q, Artamonov M, Ho T, Rabitz H (2005) J Chem Phys 122:084110
9. Ren Q, Balint-Kurti GG, Manby FR, Artamonov M, Ho T, Rabitz H (2006) J Chem Phys 124:014111
10. Balint-Kurti GG, Zou S and Brown A (2008) Adv Chem Phys 138:43–94
11. Shapiro M, Brumer P (1992) Ann Rev Phys Chem 43:257–282
12. Gross P, Singh H, Rabitz H, Mease K, Huang GM (1993) Phys Rev A 47:4593–4604
13. Sharma S, Sharma P, Singh H (2007) J Chem Sci 119:433–440
14. Kumar P, Singh H (2007) J Chem Sci 119:441–447
15. Kumar P, Sharma S, Singh H (2008) J Theo Comput Chem 7 (in press)
16. Peirce AP, Dahleh MA, Rabitz H (1998) Phys Rev A 37:4950–4964
17. de Vivie-Riedle R, Troppmann U (2007) Chem Rev 107:5082–5100
18. Meier C, Heitz MC (2005) J Chem Phys 123:044504
19. Ventalon C, Fraser JM, Vos MH, Alexandrou A, Martin JL, Joffre M (2004) Proc Natl Acad Sci U S A 101:13216–13220

20. Abe M, Ohtsuki Y, Fujimara Y, Domcke W (2005) J Chem Phys 123:144508
21. Singh H, Sharma S, Kumar P, Harvey J, Balint-Kurti GG (2008) Lec Notes in Comp Sc 5102:387–395
22. Nibbering ETJ, Dreyer J, Kuhn O, Bredenbeck J, Hamm P, Elsaesser T (2007) Vibrational dynamics of hydrogen bonds, Springer series in chemical physics. Springer Berlin Heidelberg 87:619–687
23. Ohmura H, Nakanaga T (2003) J Photochem Photobiol A: Chem 158:69–76
24. Lami A, Villani G (2007) Theor Chem Acc 117:755–764
25. Villani G (2005) Chem Phys 316:1–8
26. Villani G (2006) Chem Phys 324:438–446
27. Šponer J, Jurečka P, Hobza P (2004) J Am Chem Soc 126:10142–10151
28. Frisch MJ et al. (2003) Gaussian03 revison B.05 Gaussian Inc Pittsburgh PA
29. Feit MD, Fleck Jr JA (1983) J Chem Phys 78:301–308
30. Feit MD, Fleck Jr JA (1984) J Chem Phys 80:2578–2584
31. Marston Clay C, Balint-Kurti GG (1989) J Chem Phys 91:3571–3578